JOURNAL OF MATERIALS SCIENCE 24 (1989) 462–470

Formation of mixed TiC/Al_2O_3 layers and α- and κ-Al_2O_3 on cemented carbides by chemical v[illegible]our d[illegible]osition

C. COLOMBIER*, B. LUX
Institute for Chemical Technology of Inorganic Materials, Technical University Vienna, Getreidemarkt 9, A-1060 Vienna, Austria

Al_2O_3 and Ti(C, O) were codeposited as a mixed chemical vapour deposition (CVD) layer from $AlCl_3$–$TiCl_4$–CH_4–CO_2–H_2 gas mixtures on cemented carbides and pure alumina substrates. A thermodynamical approach of this CVD system is presented. The coatings were described by SEM and X-ray diffraction analysis. They consist of large facetted α-Al_2O_3 crystals containing some titanium and surrounded by a fine grained Ti(C, O) matrix. Carbon diffusing from the cemented carbide substrate can considerably influence the morphology and the composition of the mixed coating.

Methane in a $AlCl_3$–CO_2–H_2 environment stabilizes the κ-Al_2O_3 phase which can be deposited as a compact layer without whisker formation on a WC–Co substrate even without a TiC underlayer.

1. Introduction

Today, most cemented carbide tools for steel cutting are coated with thin layers (up to 10 μm) of refractory materials e.g. TiC, TiN, Ti(C, N), Al_2O_3, HfN, etc., in order to improve their wear resistance [1]. Many of these coatings are applied as multilayers, i.e. a succession of layers of different materials one above the other permitting optimization of the coating's technological properties. One important feature of multilayers alternating several TiC, Al_2O_3 or TiN layers is their particularly fine grain size, independent of the overall coating thickness. Fig. 1 gives an example of coatings similar in thickness and chemical composition but very different in their morphology. In both cases the coating consists mainly of alumina deposited on a cemented carbide substrate. In the first case (Fig. 1a) the coarse Al_2O_3 crystals grew during a normal chemical vapour deposition (CVD). In the second case (Fig. 1b) the Al_2O_3 growth was disrupted by a very thin TiC layer resulting in a substantial grain refinement in the Al_2O_3 layer. Fine grained coatings can be particularly advantageous for certain metal cutting applications as far as tool life and performance are concerned.

The aim of this work is to study in more detail the possibilities of combining two refractory materials within a coating in a different way. This will not be done as a "multilayer" but as a "mixed layer", i.e. the deposition of both phases occurs simultaneously side by side in a compacted layer.

Such CVD codeposition systems have already been described in the literature. For example Stinton *et al.* [2] deposited SiC–$TiSi_2$ "ceramic–ceramic composite layers" and Hirai *et al.* [3] mixed Si_3N_4–BN coatings. The thermodynamics of the latter CVD system was studied in detail by Besmann [4]. Such calculations, used instead of the experimental trial-and-error methods, allow a considerable reduction in the experimental effort which can then be devoted to the kinetics of CVD reactions only.

2. Thermodynamic approach

Thermodynamic calculations based on the minimization of the total Gibbs free energy of a system were carried out using the computer programs "Freemin" and "Ekvicalc" [5]. In accordance with earlier experimental deposition conditions, calculations were performed for 1050° C and 65 mbar only for the systems containing aluminium, titanium, oxygen, carbon, chlorine and hydrogen.

More than 40 condensed phases and 120 gases were considered. The results are represented in Fig. 2 as thermodynamic yields of the deposited solid phases TiC, Al_2O_3, C, Ti_2O_3 and Ti_3O_5 according to the following equations

$$Y(TiC) = \frac{\text{mole TiC equil}}{\text{mole } TiCl_4 \text{ inlet}} \cdot 100$$

$$Y(Al_2O_3) = 2 \cdot \frac{\text{mole } Al_2O_3 \text{ equil}}{\text{mole } AlCl_3 \text{ inlet}} \cdot 100$$

$$Y(C) = \frac{\text{mole C equil}}{\text{mole } CH_4 \text{ inlet}} \cdot 100$$

$$Y(Ti_2O_3) = 2 \cdot \frac{\text{mole } Ti_2O_3 \text{ equil}}{\text{mole } TiCl_4 \text{ inlet}} \cdot 100$$

* *Present address*: Atochem, Centre de Recherche Rhône Alpes, Bp 20, F-69310 Pierre-Bénite, France.

0022–2461/89 $03.00 + .12

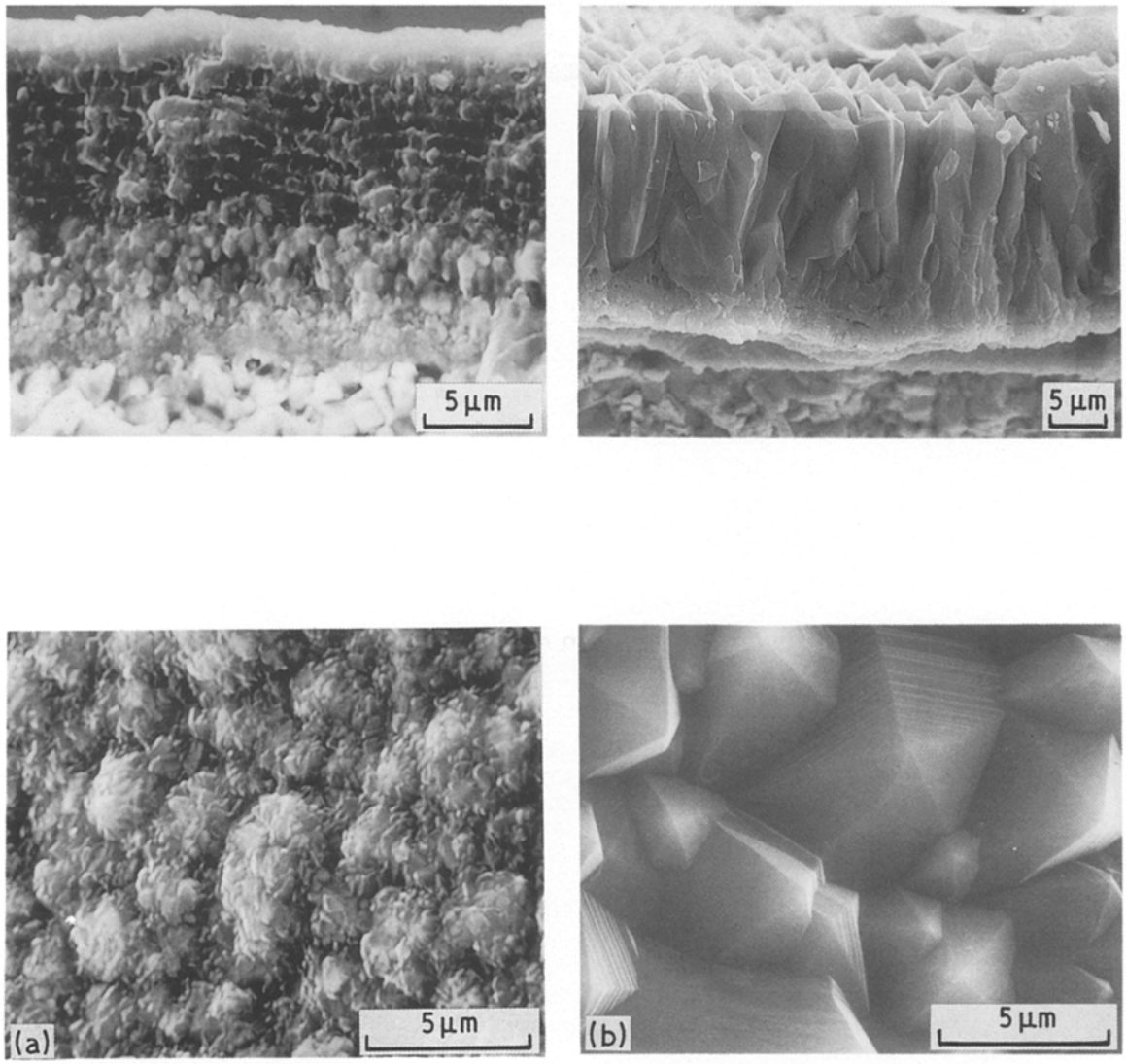

Figure 1 Comparison of the grain size in thick alumina CVD coatings deposited on WC–Co–TiC substrates. (a) Al_2O_3–TiC multilayer. The alumina deposition was briefly interrupted by a thin TiC deposition made without flushing the reactor wall between the two CVD processes. The result was a very fine grained Al_2O_3 coating. (b) Pure Al_2O_3 layer. As is generally the case in CVD systems applied to uniform crystalline layers, the crystallites grew in size during deposition because of the low nucleation frequency. The coating has a columnar structure with large alumina crystallites.

$$Y(Ti_3O_5) = 3 \cdot \frac{\text{mole } Ti_3O_5 \text{ equil}}{\text{mole } TiCl_4 \text{ inlet}} \cdot 100$$

Fig. 2 shows the influence of the $AlCl_3$, CH_4 and CO_2 concentrations in the gas phase on the solid deposits as obtained by the calculations. In the absence of CH_4, deposition of Ti_2O_3 can be avoided at $AlCl_3$ concentrations greater than 1.8 mol %. In the absence of $AlCl_3$ the Ti_2O_3 deposition should not occur if the CH_4 concentration exceeds 3.7 mol %. At high $AlCl_3$ and CH_4 concentrations (3 and 6 mol % respectively) the CO_2 concentration has to be low enough (less than 7.7 mol %) to prevent Ti_3O_5 formation.

It must be noted however that these calculations were performed assuming formation of pure solid phases. The solubility of elements in solids, i.e. mixed crystal formations such as Ti(C, O), etc., could not be considered with the computer program.

3. Experimental methods

3.1. CVD procedures

In a small CVD apparatus (Fig. 3) gas mixtures of $TiCl_4$, $AlCl_3$, CH_4, CO_2 and H_2 could be produced. $TiCl_4$ was evaporated and $AlCl_3$ was prepared *in situ* by reacting dried HCl with hot aluminium chips (350° C), both at a pressure of one atmosphere. Seven samples could be simultaneously coated in the "hot Wall" reactor. For the exact arrangement of the reactor chamber [6]. All CVD experiments were carried out for 1 h at 65 mbar total pressure and 1050° C. The flow rate was 40 l h^{-1} (diameter) of the reactor tube: 2.5 cm). The composition of the gas phase for each experiment is indicated in Table I.

In accordance with the results of the thermodynamic study, high $AlCl_3$ concentrations (3 mol %) and high CH_4 concentrations (6 mol %) were chosen in order to avoid titanium oxide formation. As already discussed by Vandelbulk [7], due to the slow kinetics of the methane decomposition, even at CH_4 concentrations above 3.7 mol % in the gas phase, no carbon deposition occurred.

The most important variable experimental parameter was the CO_2 concentration, which was varied from 0 to 2 mol %. This parameter can be considered as a critical one, since experimental conditions must be

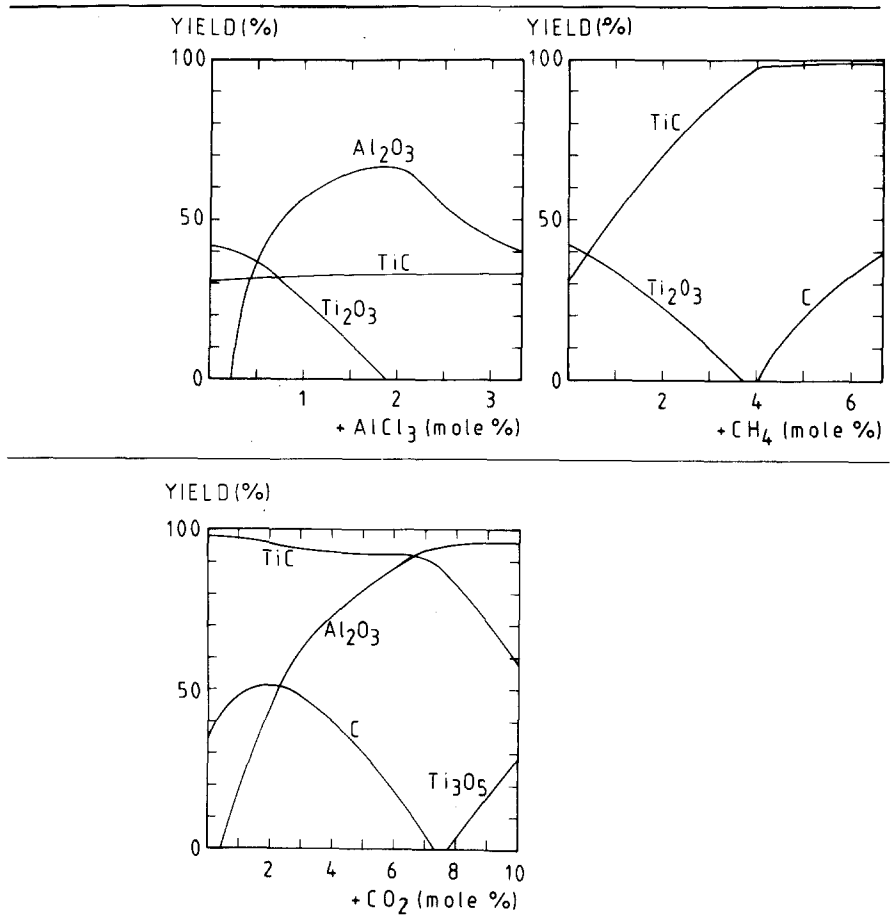

Figure 2 Thermodynamic calculations in the $TiCl_4$–$AlCl_3$–CH_4–CO_2–H_2 CVD systems. Influence of the $AlCl_3$ and CH_4 concentrations (in the presence of 3 mol % $TiCl_4$ and 1 mol % CO_2) and of the CO_2 concentration (in the presence of 3 mol % $TiCl_4$, 3 mol % $AlCl_3$ and 6 mol % CH_4) on the yield of the deposited substances (1050° C, 65 mbar, hydrogen carrier gas).

$$Y(\mathrm{TiC}) = \frac{\text{mole TiC eq}}{\text{mole } TiCl_4 \text{ in}} \times 100, \quad Y(Al_2O_3) = \frac{\text{mole } Al_2O_3 \text{ eq}}{\text{mole } AlCl_3 \text{ in}} \times 100,$$

$$Y(\mathrm{C}) = \frac{\text{mole C eq}}{\text{mole } CH_4 \text{ in}} \times 100, \quad Y(Ti_2O_3) = 2 \times \frac{\text{mole } Ti_2O_3 \text{ eq}}{\text{mole } TiCl_4 \text{ in}} \times 100,$$

$$Y(Ti_3O_5) = 3 \times \frac{\text{mole } Ti_3O_5 \text{ eq}}{\text{mole } TiCl_4 \text{ in}} \times 100$$

found for which titanium oxidation is kept at an absolute minimum.

3.2. Substrates

The substrates used were

(i) polycrystalline sintered corundum with a polished surface (0.01 μm surface roughness)

(ii) cemented carbides containing WC, TiC, TaC, NbC and Co uncoated or coated with 6 μm TiC (referred to below as "WC–Co" or "WC–Co/TiC").

3.3. Adhesion test

For the characterization of the adhesion, the coatings were tested as follows. At the beginning the coated surface of the sample was simply scratched with a tungsten carbide needle by hand. However, observation with the light microscope or SEM did not permit the clear distinction between spalling off or simple grooving of the coated surface.

Thus it was necessary to rub a spherical crater through the coating by erosion using a steel ball and

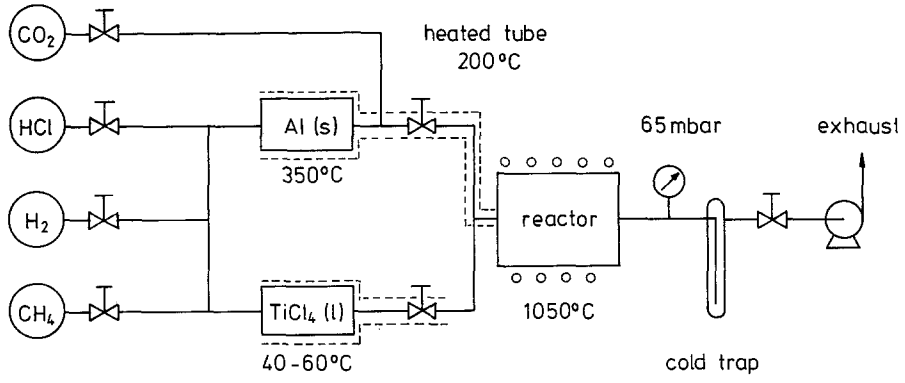

Figure 3 Schematic illustration of the apparatus used for deposition of Al_2O_3–TiC multilayers and mixed layers.

TABLE I Influence of the gas phase and the substrate on the nature of the phases deposited by CVD from $TiCl_4$–CH_4–$AlCl_3$–CO_2–H_2 (gas mixtures hydrogen as carrier gas). 1050° C and 65 mbar total pressure.

Run	Composition of the gas phase (mol %)				Deposited phases depending on the nature of the substrate		
	$TiCl_4$	CH_4	$AlCl_3$	CO_2	α-Al_2O_3	WC–Co/TiC	WC–Co
1	0	0	3	1	α-Al_2O_3	α-Al_2O_3	α-Al_2O_3
2	3	0	3	1	α-Al_2O_3	α-Al_2O_3 TiC_xO_y	α-Al_2O_3 TiC_xO_y
3	0	6	3	1	α-Al_2O_3	κ-Al_2O_3	κ-Al_2O_3
4	3	6	0	0	TiC	TiC	TiC
5	3	6	3	0	TiC	TiC	TiC
6	3	6	3	0.5	TiC_xO_y	TiC_xO_y	α-Al_2O_3 TiC_xO_y
7	3	6	3	0.7		α-Al_2O_3	
8	3	6	3	1		$+TiC_xO_y$	
9	3	6	3	2	α-Al_2O_3		

a diamond suspension at the site where the scratch had been made earlier.

This procedure permitted the viewers, by examination with an optical microscope, to judge the quality of the adhesions (Fig. 4). It could be easily seen whether or not the layer had been removed by the tungsten carbide needle. A more detailed description of the ball cratering technique is in the literature [8, 9].

3.4. SEM

The morphologies of the coatings were examined by SEM after a sputtered deposition of a thin gold layer.

4. Results

4.1. X-ray diffraction analyses

Tables I and II indicate the solid phases deposited after the CVD reaction on each of the substrates for several gas phase compositions.

The comparison between runs 1 and 3 in Table I shows that 6 mol % CH_4 led to the formation of the κ-Al_2O_3 phase instead of the α-Al_2O_3 phase.

However, on a pure α-Al_2O_3 (corundum) substrate the κ-modification was never deposited. SEM images showed that on these substrates a perfect epitaxial growth of the α-alumina phase took place instead. While in the case of cemented carbide substrates methane obviously favoured the formation of κ-Al_2O_3, the epitaxial growth conditions forced the α-Al_2O_3 (corundum) modification to grow on an α-Al_2O_3 substrate.

It should be mentioned that α-Al_2O_3 was also always observed if the high purity $AlCl_3$–CO_2–H_2 system was applied on both cemented carbide and Al_2O_3 substrates. However, it is known that certain impurities can enhance the κ-alumina formation on cemented carbide substrates [10].

If during the Al_2O_3 deposition both methane and $TiCl_4$ are present (runs 6 to 9, see Table I) α-alumina is again the only phase to be formed on both substrates, showing that $TiCl_4$ stabilizes α-Al_2O_3 more than κ-Al_2O_3. The reason for this is probably that Ti_2O_3 has the same crystal structure, trigonal scalenoedric, as α-Al_2O_3.

In all cases where $TiCl_4$ and CO_2 were present simultaneously, even with low CO_2 concentrations, a cubic titanium oxicarbide phase was formed. Even the presence of $AlCl_3$ cannot prevent — by the formation of the stable Al_2O_3 — the incorporation of oxygen in the TiC. This, however, is not necessarily detrimental for the cutting properties of the tool: good wear resistance has been reported for titanium–oxicarbid layers by Kikuchi *et al.* [11, 12].

As shown in Table II, depending on the deposition conditions, two main Ti(C, O) compositions were formed. In all cases the oxygen-rich composition was observed if CO_2 was present. The carbon-rich composition could only be observed on substrates containing carbon, particularly in the WC–Co substrates without a TiC coating. Obviously and in accordance with Kikuchi *et al.* [12] carbon diffusion from the substrate enhances the carbon content of the Ti(C, O) phase.

The exact compositions of these oxicarbide phases are difficult to determine from the lattice parameters

TABLE II Influence of CO_2 concentration and substrate on the composition of the deposited titanium oxicarbide phases.

Substrate	CO_2 concentration in the gas phase (mol %)				
	0	0.5	0.7	1	2
α-Al_2O_3	TiC	$TiC_{0.2}O_{0.8}$	$TiC_{0.2}O_{0.8}$	TiC_xO_y broad and weak peaks	not observed
WC–Co/TiC	TiC	$TiC_{0.65}O_{0.35}$ $TiC_{0.2}O_{0.8}$	$TiC_{0.2}O_{0.8}$	$TiC_{0.2}O_{0.8}$ broad and weak peaks	TiC_xO_y broad and very weak peaks
WC–Co	TiC	$TiC_{0.65}O_{0.35}$ $TiC_{0.2}O_{0.8}$	$TiC_{0.65}O_{0.35}$ $TiC_{0.2}O_{0.8}$	$TiC_{0.65}O_{0.35}$ $TiC_{0.2}O_{0.8}$	TiC_xO_y

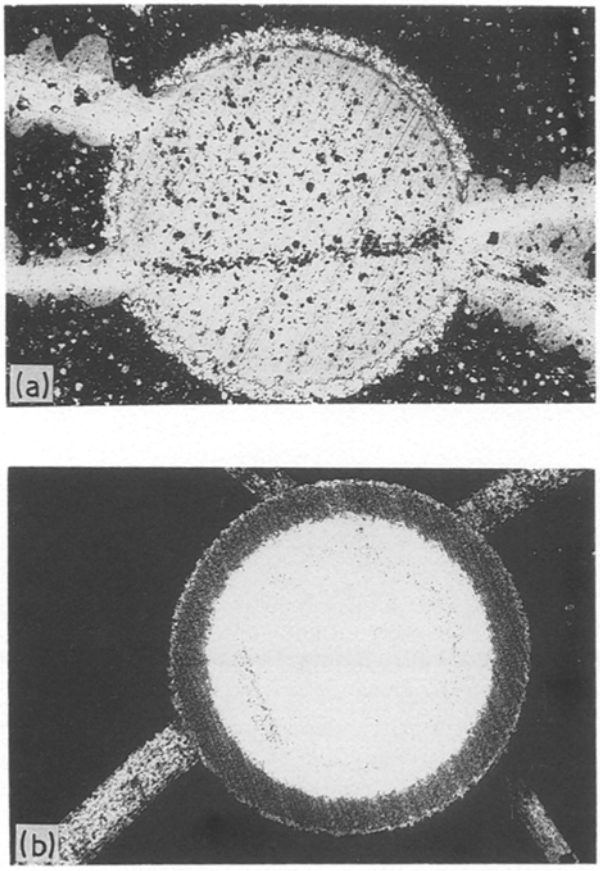

Figure 4 Adhesion test. (a) Pure TiC layer on pure Al_2O_3 substrate: poor adhesion. (b) TiC–Al_2O_3 composite layer on a WC–Co–TiC substrate: good adhesion.

as they are influenced by both elements, carbon and oxygen, and by the overall stoichiometry, which cannot be measured in a simple way. From the work of Neumann *et al.* [13] and with the assumption that stoichiometric compositions were reached, the main compositions should be $TiC_{0.65}O_{0.35}$ and $TiC_{0.2}O_{0.8}$ respectively.

The formation of the two different Ti(C, O) compositions can be interpreted as a result of two different carbon sources in the CVD system.

(1) The hard metal substrates and especially those not coated with TiC can deliver carbon by diffusion to the interface were deposition takes place.

(2) The methane in the gas phase is the second source of carbon.

According to this assumption, the carbon-rich compositions can be formed only if the two carbon sources act simultaneously, that is, if they deliver enough carbon for its stabilization. This did not occur at all on alumina substrates (see Table II).

From the work of Belon and Forestier [14], the determination of the lattice parameters allowed the evaluation of the titanium concentration in the α-Al_2O_3 phase. The maximal Ti_2O_3 concentration in α-Al_2O_3 is near 12.5 wt % [14]. In our experiments the titanium concentration in α-Al_2O_3 was greater for higher CO_2 additions (Table III). This can be explained by the increased growth rates of the alumina in these cases. It is well known that a high growth rate favours the incorporation of trace impurities into a growing crystal [15, 16].

TABLE III Influence of the CO_2 concentration on the Ti_2O_3 content in the α-Al_2O_3 phase

CO_2 (%)	lattice parameters of α-Al_2O_3	Ti_2O_3 wt %
0.5	not measurable	
0.7	4.7603	$\simeq 1\%$
1	4.7603	$\simeq 1\%$
2	4.7652	$\simeq 7\%$

4.2. Adhesion of the coatings

All coatings exhibited good adhesion on all substrates with one exception, the coating–substrate combination of a pure TiC coating on a pure and polished α-Al_2O_3 substrate, which showed poor adhesion (see Fig. 4). This was surprising since SEM investigations showed that TiC grew epitaxially on the α-Al_2O_3 substrates. Epitaxy is, therefore, not necessarily the only criterion for good adhesion of a coating. Other factors such as chemical compatibility or relative thermal expansion coefficients or monoatomic impurity layers are probably just as important. The results obtained in the present work show that, from the view-point of the adhesion only, it seems preferable to coat alumina with titanium oxicarbide rather than with pure TiC.

5. Microstructure of the coatings

A typical layer morphology is shown in Fig. 5. The TiC_xO_y and Al_2O_3 phases can be easily distinguished by EDX analyses. The Al_2O_3 grains have faceted hexagonal (0001) planes and a rough surface on the prismatic crystal faces. The mechanism of crystal growth is different depending on the orientation. The growth rates however remain similar in both crystal directions since no whiskers or needles are formed. The TiC_xO_y phase acts as a matrix for the alumina grains and is particularly fine grained.

5.1. Influence of the CO_2 concentration

Higher CO_2 concentrations provoke a higher Al_2O_3 nucleation frequency (Fig. 6). With 2% CO_2 small Al_2O_3 crystals touching each other to form a columnar structure are observed. The TiC_xO_y phase is present as a "binder" between the columnar alumina grains.

5.2. Influence of the carbon diffusion from the substrate on the coating formation

In order to study the influence of carbon diffusion from the substrate as well as the layer formation on three different substrates under methane-free deposition conditions in the gas phase (run 2, see Table I), the following three substrates were coated (see Fig. 7).

(1) α-Al_2O_3 substrates: No carbon in the substrate; only a compact α-Al_2O_3 coating containing titanium is formed.

(2) WC–Co substrates with a CVD TiC underlayer: The TiC layer acts as a diffusion barrier for the carbon from the cemented carbide substrates. α-Al_2O_3 and TiC_xO_y grow in combined formations. The α-Al_2O_3 grains are not agglomerated as in the case of the alumina substrate.

(3) WC–Co substrate: Carbon can diffuse easily from this substrate to the growing interface. The same phases as in (2) are formed, but the Al_2O_3 deposition

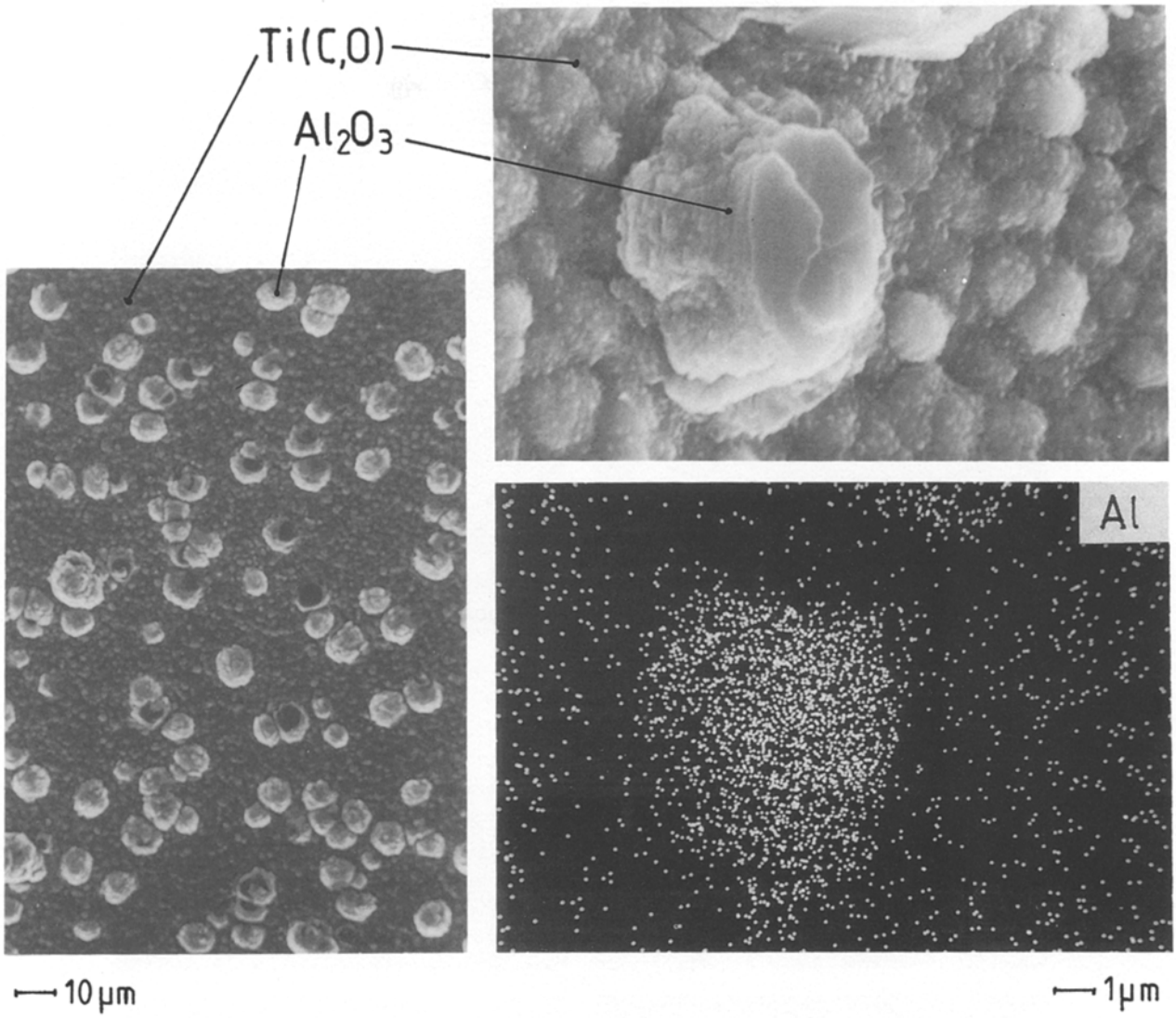

Figure 5 Typical mixed coating layer deposited from a complex $TiCl_4$–$AlCl_3$–CH_4–CO_2–H_2 environment. WC–Co substrate. The Al_2O_3 and TiC_xO_y phases can be easily distinguished by EDX analyses.

is more difficult due to the easier growth of the TiC_xO_y phase. The effect is an increase of the Ti(C, O)-"binder" and a greater distance between the Al_2O_3 grains.

This comparison shows that the morphology of the coating can be considerably influenced by the carbon activity of the substrate.

For long deposition times, the Al_2O_3 formation should become easier and the TiC_xO_y deposition more difficult. The result would be a progressive transition from a TiC_xO_y to an Al_2O_3 phase. The formation of a composition gradient along this coating could create an ideal adhesion condition for a thick alumina layer on a substrate.

5.6. Influence of CH_4 on the Al_2O_3 deposition

From Table I only the cases 1 and 3, where $TiCl_4$ was not present in the gas phase and where only Al_2O_3 phases are formed, are discussed.

It was shown in Section 4.1 that CH_4 leads to the formation of a κ-Al_2O_3 phase. Another important effect was the difference in morphology of the coatings on a cemented carbide substrate without a prior TiC–CVD coating (see Fig. 8). It is known that deposition of alumina on an uncoated cemented carbide substrate is more difficult due to reactions of the cobalt binder with the gas environment, leading to the formation of volatile $CoCl_2$ [17, 18]. It was shown recently that the deposition of alumina layers on such cemented carbide substrates is easier if aluminium bromide or aluminium iodide were used instead of aluminium chloride as the aluminium-donor in the gas phase [18].

In the chloride environment, the volatile chloride impurities led to the growth of Al_2O_3 whiskers (Fig. 8a). Additional methane in the gas phase was in this case beneficial since a compact Al_2O_3 layer was the result (Fig. 8b). There are two possible reasons.

(1) Although $CoCl_2$ did not markedly influence the growth mode for the κ-alumina crystals, it did in the α-phase, leading to the formation of α-Al_2O_3 needles.

(2) CH_4 decomposition increased the carbon activity in the cobalt phase at an early stage in the CVD. Since tungsten was also present in the cobalt-binder, precipitation of WC could occur. A very thin protective layer of WC at the cobalt-binder surface thus formed at an early stage of the CVD process, hindering the reaction between cobalt and the chlorides of the gas phase.

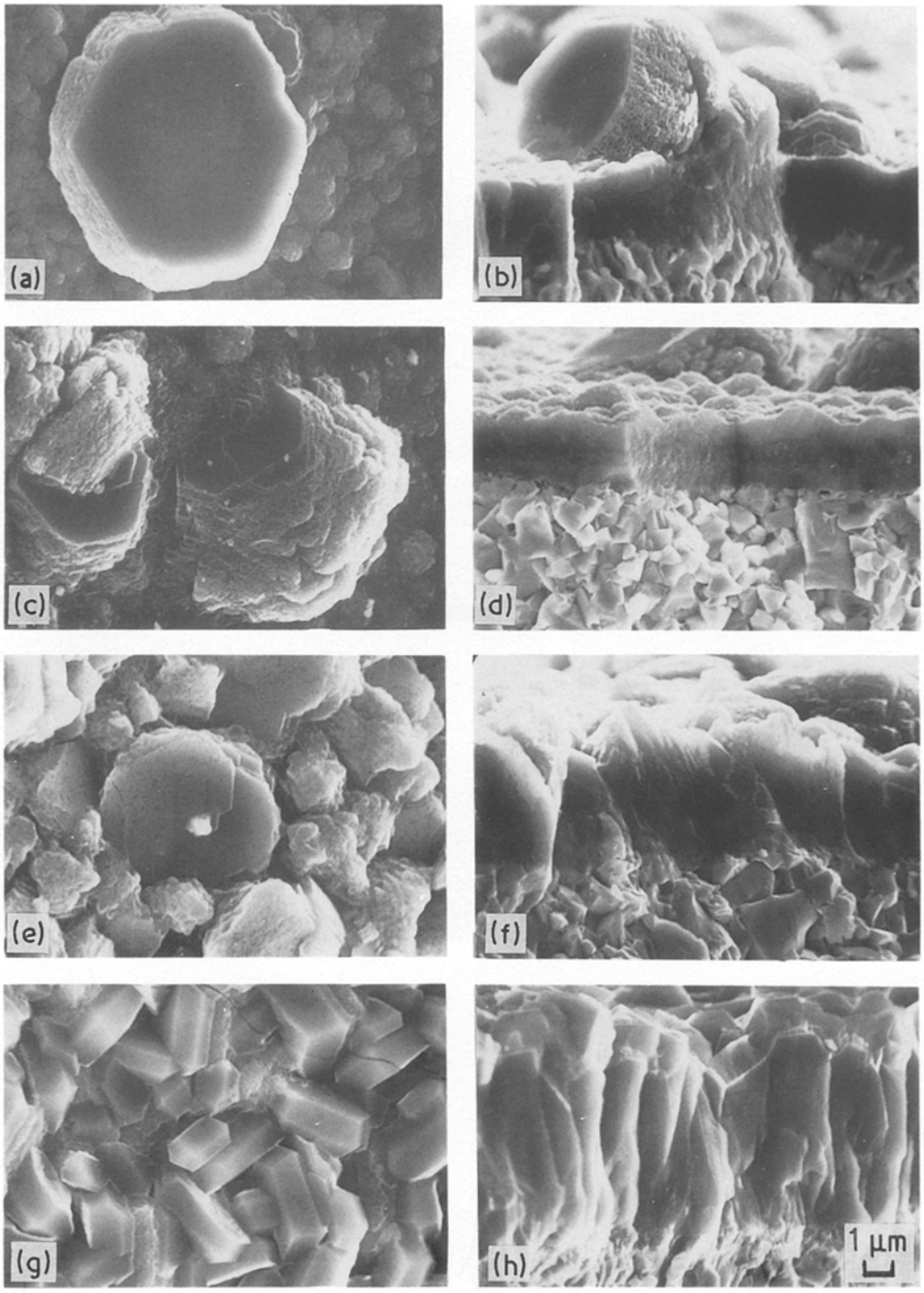

Figure 6 Influence of the CO_2 concentration on the coating morphology in the Al_2O_3–TiC CVD codeposition system at 1050° C and 65 mbar. $AlCl_3$–$TiCl_4$–CH_4–CO_2–H_2: 3–3–6–x–(88–x) mol %. (a) Surface 0.5 mol % CO_2, (b) fracture 0.5 mol % CO_2, (c) surface 0.7 mol % CO_2, (d) fracture 0.7 mol % CO_2, (e) surface 1 mol % CO_2, (f) fracture 1 mol % CO_2, (g) surface 2 mol % CO_2, (h) fracture 2 mol % CO_2.

6. Conclusion

Mixed compact CVD coatings can be deposited from $AlCl_3$–$TiCl_4$–CO_2–CH_4–H_2 gas phases at 1050° C and 65 mbar total pressure. The coatings consist of relatively large, faceted α-Al_2O_3 crystals containing some titanium and surrounded by a fine grained titanium oxicarbide matrix. Two main titanium–oxicarbide compositions were found. Their formation depends on the nature of the carbon donor. If only CH_4 acts as a carbon source, a $TiC_{0.2}O_{0.8}$ phase is formed. If the carbon is delivered by diffusion from the substrate, a $TiC_{0.65}O_{0.35}$ phase is formed.

As carbon diffusion from the substrate decreases, with increasing coating thickness more and more of the alumina deposit is formed. It therefore seems possible to obtain a progressive transition from a TiC to an Al_2O_3 deposition, thus creating optimal adhesion conditions between a thick coating and the substrate.

It is confirmed that CH_4 in an $AlCl_3$–CO_2–H_2 environment stabilizes the κ-Al_2O_3 phase, which can be deposited as a compact layer without whisker formation on a WC–Co substrate even without a TiC underlayer.

Acknowledgements

The authors thank Sandvik AB, Stockholm for supplying specimens, for helpful discussions to members of the R&D team of the Coromant division and the

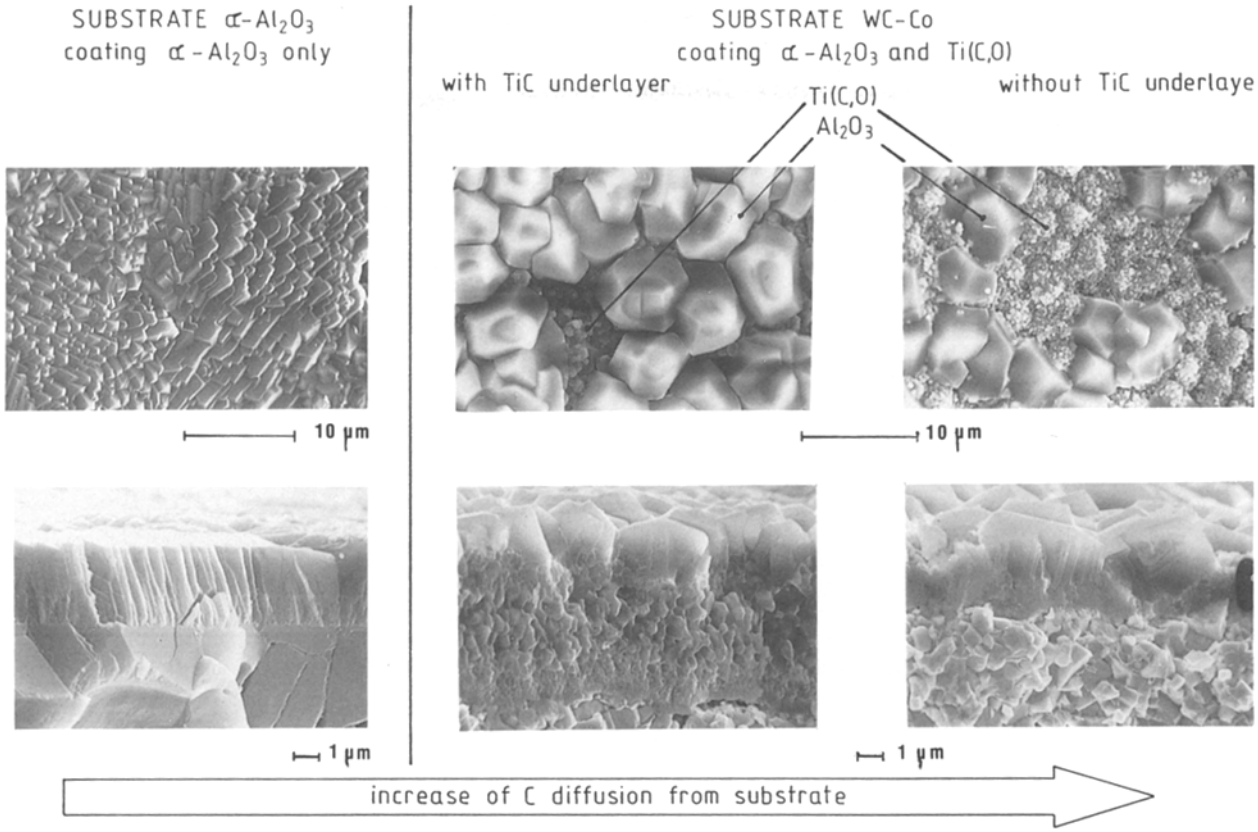

Figure 7 Influence of the carbon diffusing from the substrate on the Al_2O_3–TiC_xO_y coating morphology. Methane was not present in the gas phase. $AlCl_3$–$TiCl_4$–CO_2–H_2: 3–3–1–93 mol %.

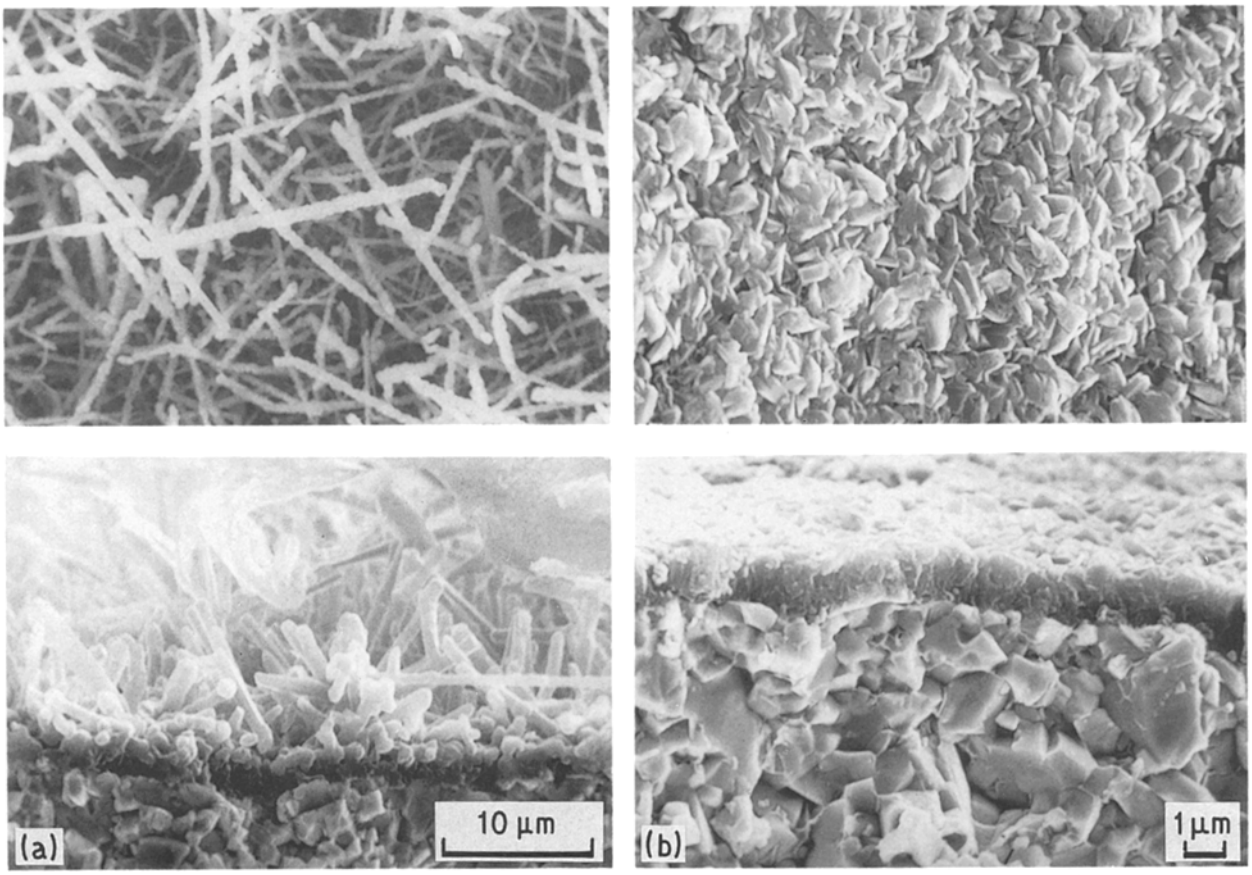

Figure 8 Influence of CH_4 on the Al_2O_3 CVD deposition. WC–Co substrate. (a) Absence of CH_4: formation of α-alumina needle crystals (b) presence of CH_4: formation of a compact κ-Al_2O_3 layer.

Austrian National Board for the Advancement of Research (Fonds zur Förderung der Wissenschaftlichen Forschung) for financial support under project S4312.

References

1. B. LUX, C. COLOMBIER, H. ALTENA and K. STJERNBERG, *Thin Solid Films* **138** (1984) 49.
2. D. STINTON, W. LACKEY, R. LAUF and T. BESMANN, *Ceram. Eng. Sci. Proc.* **5** (1984) 668–76.
3. T. HIRAI, T. GOTO and T. SAKARI, Emergent Process Methods for High Technology Ceramics, R. Davis, H. Palmour and R. Porter (Eds) (Plenum Press, New York, 1982) pp. 347–358.
4. T. BESMANN, *J. Amer. Ceram. Soc.* **69** (1986) 68–74.
5. B. NOLÄNG, Proceedings of the 5th European Conference on CVD, Uppsala, 107 (1985).
6. C. COLOMBIER, PhD thesis, Technical University of Vienna (1984).
7. L. VANDENBULK, Proceedings 8th International Conference on CVD, the Electrochemical Society, Pennington, 3 (1981).
8. H. BOVING and R. ROCCHI, 53. eme Congress Soc. Suisse de Chronometrie, La Chaux de Fonds, 507 (1978).
9. C. COLOMBIER, B. LUX, A. RIAHI, M. PUCHHAMMER and H. STÖRI, *Anal. Fresenius Z. Chem.* **329** (1987) 355–360.
10. J. LINDSTRÖM and U. SMITH, European Patent 0045291 Al, July (1981).
11. N. KIKUCHI, Y. LYZUKI, T. SUGIZAWA and F. WASHIZU, US Patent 4 341 834 (1982).
12. N. KIKUCHI, H. DOI and T. ONISHI, Proceedings 6th International Conference on CVD, 403 (1977).
13. G. NEUMANN, R. KIEFFER and P. ETTMAYER, *Monatshefte für Chemie* **103** (1972) 1130.
14. L. BELON and H. FORESTIER, *C. R. Acad. Sci. Paris* **258** (1964) 4282.
15. V. G. SMITH, W. A. TILLER and J. W. RUTTER, *Can. J. Phys.* **33** (1955) 723.
16. C. FLEMINGS, "Solidification Processing" (McGraw-Hill, New York, 1974) p. 55.
17. H. ALTENA, C. COLOMBIER, A. LEBL, J. LINDSTRÖM and B. LUX, Euro CVD 4, edited by J. Bloem, G. Verspui and L. Wolff, Eindhoven, 428 (1983).
18. C. COLOMBIER, J. PENG, H. ALTENA and B. LUX, *Int. J. Refr. Hard Metals* **5** (1986) 82.

Received 19 January
and accepted 1 June 1988